geosciences

MDPI

Article

Changing Impacts of North Atlantic Tropical Cyclones on Extreme Precipitation Distribution across the Mid-Atlantic United States

Nirajan Dhakal

Environmental and Health Sciences Program, Spelman College, Atlanta, GA 30314, USA; ndhakal@spelman.edu

Received: 1 April 2019; Accepted: 7 May 2019; Published: 9 May 2019

Abstract: Almost every year, north Atlantic tropical cyclones (TCs) are responsible for significant socioeconomic losses across the Mid-Atlantic USA. However, the extent to which TC activity contributes to the changes in the probability distributions of the extreme precipitation have not yet been comprehensively characterized for this region. In this study, a quantile regression method was used to investigate the trends of the lower (τ = 0.2) and upper (τ = 0.8) quantiles of annual and seasonal daily maximum precipitation series for the region using the station-based daily precipitation data for the period 1950–2011. Results show that the rates of changes in the upper quantile have greatly strengthened for the region. Analysis of the spatial pattern of the lower and upper quantile trends for TC and non-TC extreme precipitation series shows that trends have larger magnitudes in most of the sites for TC precipitation series as compared with the non-TC precipitation series for both the lower and upper quantiles. Additionally, the highest trends are observed in the upper quantile for TC time series indicating that TC precipitation is contributing more to the upper tails of the extreme precipitation distribution as compared to the non-TC precipitation. Results from this study have implications for the improved design and reassessment of flood-controlling infrastructure.

Keywords: extreme precipitation; tropical cyclones; quantile regression; distributional changes

1. Introduction

The Mid-Atlantic region of the U.S. (extending from southern New York to North Carolina and from western New Jersey to West Virginia) is known to experience a very diverse climate and a tremendous variety of weather systems including landfalling tropical cyclones, having undergone extratropical transition. Almost every year, tropical cyclones (TCs) are responsible for significant socioeconomic losses across the eastern United States including the Mid-Atlantic region. Strong winds, storm surges, heavy rainfall and flooding associated with TCs are the major threats to life and infrastructure not only in coastal areas but miles inland as well [1–5]. A recent example is the severe damages caused by tropical cyclones Harvey and Irma during the active 2017 Atlantic tropical cyclone season [6]. Similarly, in 2011, damages from tropical cyclone Irene totaled $7.3 billion and resulted in 45 deaths [7]. Although precipitation directly associated with TCs is less than 25% of the annual precipitation even in the most affected regions, the impacts in terms of extremes can be significant (e.g., [8,9].

Studies have shown that TC activity in the North Atlantic exhibits variability on intra-annual [10], interannual [11,12], and interdecadal timescales [13]. A few studies have documented an increase in the Atlantic TC activity during the latter part of the 20th century. For example, Webster [14] showed that the number of cyclones and cyclone days have increased in North Atlantic during 1990–2004; Emmanuel [15] showed that the destructiveness of TCs measured based on Power Dissipation Index (PDI) has increased remarkably since the mid-1970s for both North Atlantic and North Pacific;

Klotzbach [16] showed a large increase in tropical cyclone intensity for North Atlantic during 1986–2005; Elsner et al. [17] showed that there is a significant upward trend in the estimated life-time maximum wind speeds of the strongest TCs (99th percentile) over North Atlantic during the period 1981–2006. In this context, a pertinent question is, whether it would be possible to infer a linkage between North Atlantic TC activities and changing statistics of precipitation extremes for the Mid-Atlantic region.

Numerous previous studies have shown an increase in the heavy precipitation trends associated with TCs in the North Atlantic basins [8,9,18–20]. Most of these studies have focused on the connection between TC activity and heavy rainfall for either the entire eastern United States [8,9,19,20] or southeastern United States [18] for the past three decades (post-1980) and they have utilized peaks over a threshold to define precipitation extremes. For example, Groisman et al. [21] used a threshold of 50.8 mm to define extreme rainfall and identified all extreme rainfall events occurring within the zone of influence of each tropical cyclone over the past century for the extreme coastal regions of the southeastern United States. Zhu and Quiring [22] explored the spatial and temporal variations of TC-related extreme precipitation (defined by a threshold of 100 mm and 50 mm) in Texas using 60 years of precipitation data. More recently, Agel et al. [23] investigated the seasonal and spatial distribution of TC-related extreme precipitation (defined as top 1% of wet days) for select locations in northeastern US. However, spatio-temporal variability of block maximum precipitation series (annual or seasonal) arising from TC have not yet been comprehensively characterized only for the Mid-Atlantic region. Block maximum series are normally used for hydrologic design based on frequency analysis (for example, [24]). Previous studies looking at the impact of TCs on precipitation changes used parametric approaches such as fitting least-squares linear regression models to look at the mean trends of precipitation indices [20]. Under warmer climates, the probability distribution function (PDF) of precipitation is expected to change [25], and hence it is useful to look at the changes in not only mean but across all thresholds of the PDF of extreme precipitation. None of these studies have specifically focused on the extent to which TC precipitation contributes to changes in the (upper or lower) tails of the overall extreme precipitation distribution.

To this end, I use a quantile regression method [26,27] to detect and identify the contribution of the TC-induced precipitation in trends of the different thresholds of the probability distribution function (PDF) of the daily annual and seasonal maximum precipitation series for the Mid-Atlantic region. Two critical advantages of using the quantile regression method are: i) it does not make distributional assumptions, and ii) it can estimate slopes of changes in all parts of the PDF of a time series [28]. To my knowledge, only one previous study used a quantile regression method to study trends in TC-induced precipitation. Ying et al. [29] applied a quantile regression method to explore trends in TC-induced wind and precipitation for China. However, this study is the first attempt to link the trends in the different thresholds of the distribution of extreme precipitation series with the TC activities for the Mid-Atlantic region. It is important to point out that TC rainfall contribution is spatially unique to each area affected by TC phenomena [30]. Therefore, understanding the spatial distribution and temporal characteristics of TC-linked extreme precipitation is important for managing the risk of extreme precipitation.

2. Materials and Methods

2.1. Study Area

The Mid-Atlantic region is one of the most extensively developed regions in the world, characterized by the presence of high-density urban areas [31]. The region has distinct physiographic features in the southern region and northern region that impacts the climate of the region: the southern states are of relatively low elevation and warmer as compared to the northern states [32]. No singular common definition for the boundaries of the Mid-Atlantic region is available. For this study, the regional boundaries specified by Polsky et al. [32] were used, which include the states of Delaware,

Maryland, Pennsylvania, Virginia, West Virginia, the District of Columbia, New York, New Jersey, and North Carolina (see Figure 1).

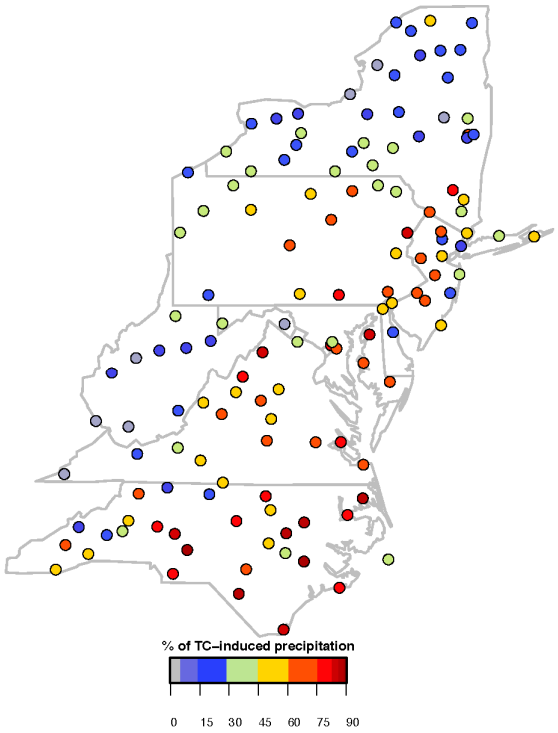

Figure 1. Spatial distribution of the percentage of top 10 TC-induced wettest days during 1950–2011.

2.2. *Data and Statistical Methods*

2.2.1. Data

Daily precipitation records for the 1950–2011 period were obtained from the Historical Climatology Network database [33] for the Mid-Atlantic region. Using the following two screening criteria, a set of 134 stations were retained for analysis in this study: (a) percentage of missing values per year less than 10%, and (b) record length greater than or equal to 55 years. Track positions of tropical cyclones are taken from the 2011 version of the US National Hurricane Center's HURDAT dataset [34]. Daily precipitation data were used to construct extreme-precipitation series of two types for the period 1950–2011 (n = 62) for each station: i) Annual maximum daily precipitation series (ADM), and ii) seasonal maximum daily precipitation series (SDM) during the major tropical cyclone season from June 1 to October 31. ADM is the maximum value of 1-day (or 24-hr) rainfall totals within each year, and SDM is the maximum value of 1-day rainfall totals during the major tropical cyclone season from June 1 to October 31 (JJASO).

2.2.2. Quantile Regression

Trends are evaluated using a quantile regression method [26,27]. A quantile regression method approximates the quantiles of a response variable based on given predictor variables. Let Y be a random variable (extreme precipitation in our case) and τ be the quantile level. Then the τ^{th} quantile of Y, denoted by $Q_Y(\tau)$, is given by $P[Y \leq Q_Y(\tau)] = \tau$, where $\tau \in [0, 1]$. In this notation, Q_Y (0.5) is the median of the sample Y. The linear quantile regression model is given by [35]

$$Q(\tau|t) = \beta_0(\tau) + \beta_1(\tau)t + \varepsilon \quad (1)$$

where $\beta_0(\tau)$ is the intercept, $\beta_1(\tau)$ is the slope or trend coefficient, t is time in years, and ε is the error term with zero expectation. The linear quantile regression minimizes the sum of weighted absolute residuals

$$\arg\min\left|\sum_{i=1}^{n}\rho_\tau\left(y_i - X_i^T\beta\right)\right| \quad (2)$$

where n is the sample size and ρ_τ is the "check function" [35].

Slopes of trends (trend coefficients) in the lower ($\tau = 0.2$) and higher ($\tau = 0.8$) tails of distribution are extracted for both ADM and SDM. A non-parametric bootstrap method [36,37] is used to measure the significance of the trends. The original time series (ADM or SDM) was randomly resampled with replacements 1000 times and, each time, quantile regression was performed with the new sample to extract the trend coefficient. The 95% confidence interval for the uncertainty is estimated using the 97.5th and 2.5th percentile values of the trend coefficient from the 1000 estimates. The trend was significant if the trend coefficient was significantly different from zero at a significance level of 0.05 [28,38,39]. The R "quantreg" [27] package was used for computation.

2.2.3. Generalized Extreme Value Distribution

Generalized Extreme Value (GEV) distribution [40] is usually used to statistically describe extreme events [41,42]. GEV distribution has three parameters: location (μ), scale (σ) and shape (ξ). The cumulative distribution function of GEV is given by [41]:

$$F(x) = \exp\left\{-\left[1+\xi\left(\frac{x-u}{\sigma}\right)\right]^{-1/\xi}\right\} \quad (3)$$

For GEV, distribution parameters can be estimated by using different methods. They include maximum likelihood (ML) method [41,43], L-moments method and Bayesian methods [44]. These different methods have advantages and drawbacks. A "return period" based on extreme precipitation is commonly used for the hydrologic design of drainage systems by engineers and water resource managers [42]. The T year return period precipitation level is the value of precipitation occurring, on average, once in every T year [45]. For this study, GEV parameters were fitted to ADM and SDM using the maximum likelihood (ML) method. Once the GEV distribution was fitted for the data, I derived the exceedance probability (as well as non-exceedance probability) of each event of ADM and SDM.

2.3. Identification of TC-induced Precipitation

To identify extreme precipitation events induced by TCs crossing the region, I utilized a threshold of radial distance between the cyclone track and the weather station receiving the precipitation. Previous research provides guidance regarding the size of the precipitation swath produced by TCs. For example, Cry [46] considered a precipitation event to be tropical within the limits of the TC circulation ranging from under 100 km to over 800 km, depending on each storm's unique characteristics. Englehart and Douglas [47] found that in 90% of cases, the TC's precipitation occurs within 600 km from the center, and they used a 550-km radius from the center of each storm to assign surface weather stations as receiving TC-induced precipitation. In this study, a precipitation event is considered induced by a TC if the cyclone track passed within a 500-km radius of the station and the event occurred within ±1 day. In this situation, it is likely that the heavy rains were associated with the tropical storm system's circulation [8]. The 500-km criterion is an operational definition to reduce the influences of other meteorological systems such as approaching extratropical cyclones [36]. While more strict definitions of landfall could be used, the one chosen is deemed reasonable in the context of flood-inducing precipitation because even if the storm center does not pass directly over land, significant inland rainfall and flooding may still occur [37]. Previously, several other studies used the similar criteria to associate a precipitation event with TC [5,8,9,19,28,48–52].

3. Results

3.1. Spatial Pattern of TC-induced Top 10 Wettest Days

I estimated the top 10 wettest days during the observed record for each station and identified the number of TC days in those top 10 wettest days. Figure 1 shows the spatial pattern of the percentage of TC-induced precipitation in the top 10 wettest days during the study period. As expected, the coastal stations show a higher percentage of top 10 TC-induced wettest days caused by TCs as compared to inland stations; this is because TC precipitation is more likely to occur in these areas. Out of 134 stations, there were 91 (68%) stations with a percentage greater than 20; 22 (16.5%) stations with a percentage greater than 50, and six (4.5%) stations with a percentage greater than 75. It was observed that the southern states showed consistently higher top 10 wettest days caused by the TCs as compared to the northern states. For the southern states, especially Virginia and North Carolina, both coastal as well as inland sites experienced a higher number of the top 10 TC-induced wettest days. As explained by Knight and Davis [20], the reason for this observation is that being a high landfall area, storms making landfall along the Gulf Coast recurve toward this region once they become influenced by westerly flow. On the other hand, the precipitation at the northern states is more strongly impacted by the lake effect [32]. Analyses like that in Figure 1 are important as they show some indication as to how the TC impacts the upper tails of the probability distribution of extreme precipitation. To explore this further, I estimated the frequency of the TC events in ADM and SDM and present this next.

3.2. Spatial Distribution of the Frequency of TC-induced Extreme Precipitation in ADM and SDM

Using the approach presented in Section 2.2., extreme precipitation events were identified as TC or non-TC events for both ADM and SDM for all the 134 stations. To identify the impacts of the TC on the probability distribution of extreme precipitation, I estimated the frequency or the ratio of the number of precipitation events associated with TCs to the total number of events at individual stations for both ADM and SDM. Results for ADM and SDM are presented in Figure 2a,b, respectively. The spatial pattern of the frequency is similar to the spatial distribution of the percentage of the TC-induced top 10 wettest days (Figure 1). As expected, for both ADM and SDM, the values of frequency are higher for coastal sites and lower for inland sites. Frequency values range from 0.05 to 0.41 for both ADM and SDM; there were 61 (45%) stations with a frequency greater than 0.15 for ADM, and 81 (63%) stations with a frequency greater than 0.15 for SDM. Similarly, there were 34 (25%) stations with a frequency greater than 0.20 for ADM, and 57 (43%) stations with a frequency greater than 0.20 for SDM. Note that for a station where the value of frequency is 0.4, 25 out 62 events are associated with TCs. Stations along Virginia and North Carolina have comparatively higher values of frequency. Spatial distribution of the frequency of non-TC precipitation in ADM and SDM (inverse of Figure 2) was developed and presented in Appendix A (Figure A1). As expected, comparatively higher frequency values were observed for northern and inland sites. As can be seen from the above analysis, both ADM and SDM are comprised of two populations, TC and non-TC precipitation events, which likely have different statistical characteristics, owing to the seasonality, and/or distinct weather processes, and moisture pathways [53]. From a hydroclimatic perspective, an important consideration in studying temporal variability in precipitation extremes is that different causative factors, such as tropical cyclones and frontal precipitation, may exhibit differential sensitivity to climatic variability and change, thus requiring attention to sample sub-populations. At the same time, for precipitation frequency analysis (used for hydrologic design), it is necessary to consider the extreme precipitation distribution as a mixed population that weighs the individual precipitation-generating phenomenon appropriately (for example, [54]). Previously, several other studies used the "mixed distribution" of distinct flood generating mechanisms in the flood frequency analysis [55,56]. Modeling the precipitation time series using "mixed distribution" is beyond the scope of this work.

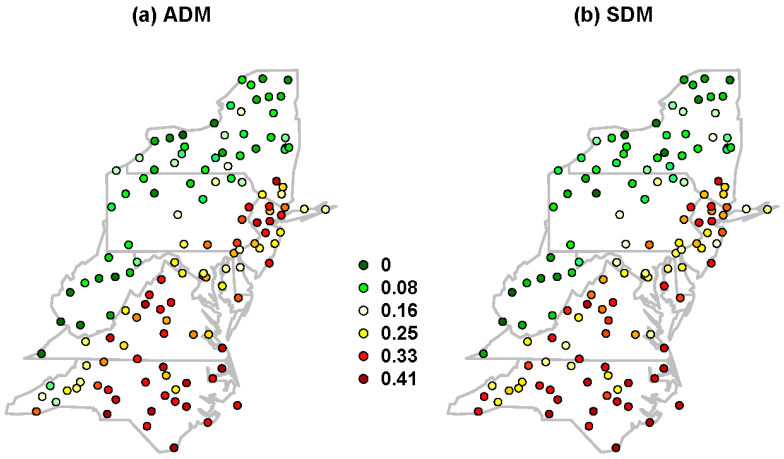

Figure 2. Frequency of extreme precipitation series associated with tropical cyclones for (**a**) ADM and (**b**) SDM.

3.3. Probability of Exceedance Based on GEV Distribution

As noted earlier, for each station, I fitted the GEV distribution to ADM (and SDM), and the exceedance probability of each precipitation event of ADM and SDM was computed based on the fitted distribution. Box plots of the non-exceedance probability (which is 1- exceedance probability) of TC and non-TC events across all stations are shown in Figure 3a for ADM and Figure 3b for SDM. Visually, it can be seen that for both ADM and SDM, non-exceedance probabilities are higher for TC events as compared to the non-TC events. The median value of the TC non-exceedance probability is 0.77, and the median value of the non-TC non-exceedance probability is 0.45 for ADM. Similarly, for SDM, the median value of the TC non-exceedance probability is 0.75, and the median value of the non-TC non-exceedance probability is 0.45. For 15% of stations, the TC non-exceedance probability is greater than 0.95 (return period of 20 years), while for only 4% of stations, the non-TC non-exceedance probability is greater than 0.95 for ADM. Similarly, for 14% of stations, the TC non-exceedance probability is greater than 0.95, while for only 3% of stations, the non-TC non-exceedance probability is greater than 0.95 for SDM. These preliminary observations (Figures 1–3) indicate that TC events occupy the upper tails of extreme precipitation distribution for the majority of the sites (for both ADM and SDM) and warrant careful identification of the relative role and impact of TCs in the extreme precipitation distribution.

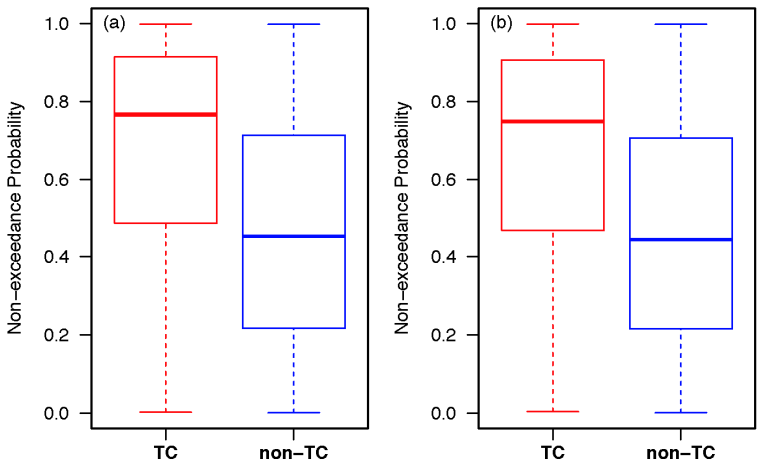

Figure 3. Box plots of the non-exceedance probability (1- exceedance probability) of TC and non-TC events across all stations for (**a**) ADM and (**b**) SDM. The non-exceedance probability was computed based on the Generalized Extreme Value Distribution fitted to ADM (or SDM) at individual station.

3.4. Trends of the Top 10 TC-Induced Wettest Days

In this section, I present an analysis of the temporal changes in the pooled estimates of total counts of the top 10 TC-induced wettest days across all 134 stations for the 1950–2011 period and presented in Figure 4. The top 10 wettest days (in terms of magnitude) were estimated for each station, each event was separated as TC and non-TC events and finally the number of times the top 10 TC-induced wettest days occurred for each year across all the sites were evaluated (represented by black dots in Figure 4). The black line shows the linear trend of the counts and the blue line shows the 10-year moving average. The linear model showed a slight increase of +0.5 per year. If we look at the variations in the count estimates represented by the moving average line, it can be seen that there has been an increase in the number of TC-induced heavy precipitation events during the post-1990 period. This is not to say that these swings are unusual; for example, the period during early- to mid-sixties also shows increases in heavy precipitation. However, not to extent seen in the recent decade. These results indicate that for the Mid-Atlantic region TC activities favor the occurrence of precipitation extremes for the recent time periods. These results support existing literature showing an increase in the heavy precipitation trends associated with TCs in the North Atlantic basins [8,9,18–20]. Additionally, these results have implications for future predictions in the context of changing climate as theoretical and modeling work predicts more TC rainfall in a warmer world in the future [57]. The bar plot in Figure 4 shows counts of the landfalling TCs for the Mid-Atlantic region during 1950–2011. As observed for the top 10 TC-induced wettest days, the counts of the landfalling TCs also show annual variability for the study period. However, the frequency of landfalling TCs has noticeably increased post-1985. The observed increase in the incidence of TC-induced heavy precipitation as well as the landfalling TCs in the recent decade leads to one pertinent question, how does this increase manifest with changes in the probability distributions and the characteristics of quantiles derived from fitted distributions of extreme precipitation? I attempt to answer this question in the subsequent sections.

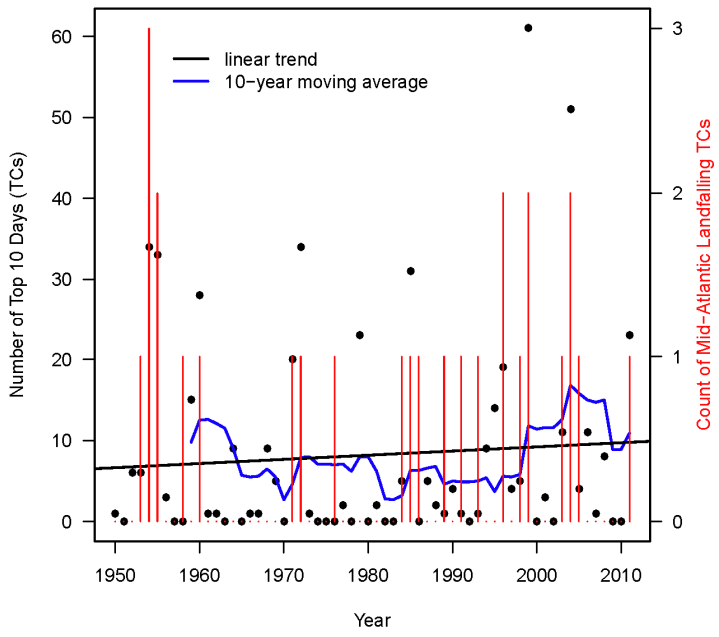

Figure 4. Trends of the counts of the top 10 TC-induced wettest days across all 134 sites; the black line shows the linear trend of the counts; the blue line shows the 10-year moving average and the red bar plot shows the counts of landfalling TCs for the Mid-Atlantic region during 1950–2011.

3.5. Spatial Patterns of Lower and Upper-Quantile Trends for ADM and SDM

In this section, I investigate the spatial patterns of the lower and upper-quantile trends of the conditional distributions of the ADM and SDM. As noted earlier, I used 20% ($\tau = 0.2$) quantile and

80% (τ = 0.8) quantile to reflect changes in the lower and upper tails of the index distribution shapes to obtain statistically stable and reliable results. Spatial patterns of the lower and upper-quantile trends for ADM are presented in Figure 5a,b, respectively. Similarly, spatial patterns of the lower and upper-quantile trends for SDM are presented in Figure 5c,d respectively. It can be seen that the lower and upper quantile trends display consistent spatial patterns across the region for both ADM and SDM. There is a clear spatial pattern associated with overall positive trends in the southern region of the study area for both the lower and upper quantiles. Slopes along the coastal sites are higher in magnitude as compared to the inland areas for both the lower and upper quantiles. However, upper-quantile trends have greater magnitudes in most of the sites as compared with the lower quantile trends. This shows that the rates of changes in the upper quantile have greatly strengthened. The strongest increasing trend in the upper quantile was observed along the coastal region of Virginia and North Carolina. In terms of significance, trends at 29 sites are statistically significant for lower quantile, and 31 sites for upper quantile for ADM. Similarly, trends at 31 sites are statistically significant for lower quantile, and 30 sites for upper quantile for SDM. Comparing Figure 5a,b with Figure 5c,d, I did not find a visible difference between the results for ADM and SDM. On the other hand, the spatial pattern of the upper quantile trends is similar to the spatial distribution of the frequency of TC-induced extreme precipitation (Figure 2). This leads to another pertinent question, whether the TC precipitation is contributing more to the changes in the upper tails of the extreme precipitation distribution as compared to the non-TC precipitation.

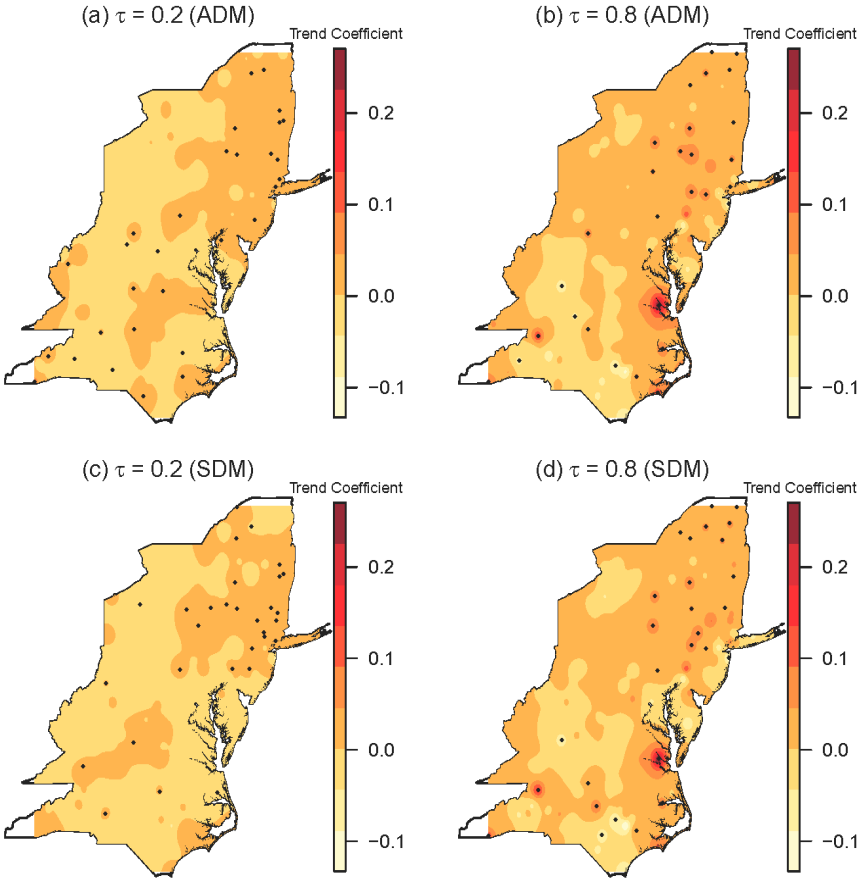

Figure 5. Analysis of the spatial patterns of lower (0.2) and upper (0.8) quantile trends of extreme precipitation for the study area; (**a**) spatial pattern of lower (0.2) quantile trends for ADM; (**b**) spatial pattern of upper quantile trends for ADM; (**c**) spatial pattern of lower (0.2) quantile trends for SDM; (**d**) spatial pattern of upper quantile trends (0.8) for SDM. Black dots represent stations with trend coefficients statistically significantly different from 0.

3.6. Contribution of TCs in the Distribution of ADM and SDM

To study the impact of TCs in the distribution of extreme precipitation, a quantile regression method was used to estimate slopes of trends in the lower quantile and upper quantiles of the TC-induced and non-TC components of ADM and SDM separately. For regression, only those stations which have at least 10 events in the ADM (or SDM) caused by TCs are used; 77 out of 134 stations were retained for analysis. The spatial pattern of the slopes are shown in Figure 6; grey circles represent those stations for which less than 10 events in ADM (or SDM) are caused by TCs; Figure 6a–d are results for ADM and Figure 6e–h are results for SDM. Figure 6a,b show the spatial pattern of the lower and upper quantile trends for TC ADM series, and Figure 6c,d show the spatial pattern of the lower and upper quantile trends for non-TC ADM series. Similarly, Figure 6e,f show the spatial pattern of the lower and upper quantile trends for TC SDM series, and Figure 6g,h show the spatial pattern of the lower and upper quantile trends for non-TC SDM series. For both ADM and SDM TC series (Figure 6a,b,e,f), there is a clear spatial pattern associated with overall positive trends (for both the lower and upper quantiles) in the coastal sites along Delaware, Maryland, Pennsylvania, Virginia, New Jersey, and North Carolina. For Virginia and North Carolina, positive trends are observed in coastal as well as inland sites for upper quantile. Slopes along the coastal sites are higher in magnitude as compared to the inland areas. Similarly, for both TC and non-TC times series, the upper quantile trends are higher as compared with the lower quantile trends, which is consistent with results from Figure 5. The trends have larger magnitudes in most of the sites for TC series as compared with the non-TC series for both the lower and upper quantiles. However, the highest trends are observed in the upper quantile for TC time series (Figure 6b,f). Comparing the results of Figure 6 with Figures 2 and 5, it can be inferred that TC precipitation is contributing more to the changes in the upper tails of the overall ADM and SDM distribution as compared to the non-TC precipitation. One major limitation of the current analysis is the small sample size of the TC events in the ADM and SDM. However, the results have implications for the improved design and reassessment of flood-controlling infrastructure.

4. Summary and Conclusions

In this study, I explored the impact of North Atlantic Tropical Cyclones (TCs) to the changes in the probability distribution of extreme precipitation for the Mid-Atlantic USA using the station-based daily precipitation data for the period 1950–2011. Extreme-precipitation series of two types, i) annual maximum daily precipitation series (ADM) and ii) seasonal maximum daily precipitation series (SDM), during the major tropical cyclone season from June 1 to October 31 were used for analysis. A quantile regression method, a fresh statistical method, was used to investigate the trends of the lower ($\tau = 0.2$) and upper ($\tau = 0.8$) quantiles of ADM and SDM. Major conclusions of this study are listed and described below:

I. Analysis of the top 10 wettest days shows that for the coastal stations, a higher percentage of top 10 wettest days is caused by TCs as compared to inland stations (Figure 1). Similarly, an analysis of the temporal changes in the counts of the top 10 TC-induced wettest days across all stations using the 10-year moving average shows that there has been an increase in the number of TC-induced heavy precipitation events during the post-1990 period (Figure 4).

II. Analysis of the spatial distribution of the frequency of TC-induced extreme precipitation in ADM and SDM shows that the values of frequency are higher for coastal sites and lower for inland sites. Stations along Virginia and North Carolina have comparatively higher values of the frequency (Figure 2).

III. Analysis of the spatial pattern of the lower and upper-quantile trends of the ADM and SDM revealed an overall positive trend in the southern region of the study area for both the lower and upper quantiles. Additionally, upper-quantile trends have greater magnitudes in most of the sites as compared with the lower quantile trends, indicating that the rates of changes in the upper quantile have greatly strengthened (Figure 5).

IV. Analysis of the impact of TCs in the distribution of extreme precipitation shows that trends have larger magnitudes in most of the sites for TC precipitation series as compared with the non-TC precipitation series for both the lower and upper quantiles. However, the highest trends are observed in the upper quantile for TC time series indicating that TC precipitation is contributing more to the changes in the upper tails of the extreme precipitation distribution as compared to the non-TC precipitation (Figure 6). This is a key finding of this manuscript.

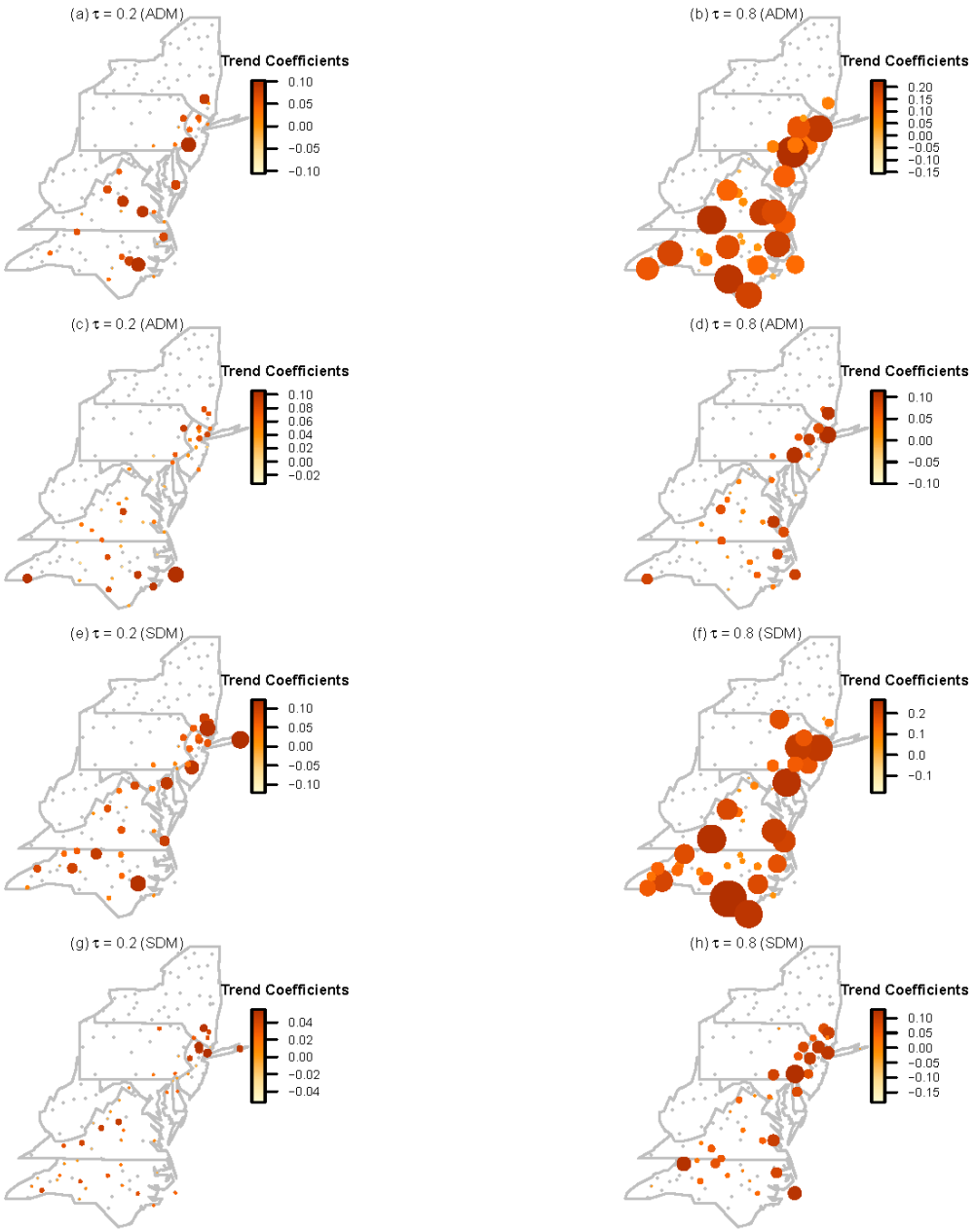

Figure 6. Analysis of the spatial patterns of lower and upper quantile trends of TC and non-TC precipitation for the study area; (**a**) spatial pattern of lower quantile trends for TC ADM series, (**b**) spatial pattern of higher quantile trends for TC ADM series; (**c**) spatial pattern of lower quantile trends for non-TC ADM series; (**d**) spatial pattern of higher quantile trends for non-TC ADM series; (**e**) spatial pattern of lower quantile trends for TC SDM series; (**f**) spatial pattern of higher quantile trends for TC SDM series; (**g**) spatial pattern of lower quantile trends for non-TC SDM series; (**h**) spatial pattern of higher quantile trends for non-TC SDM series.

One limitation of this study is the small sample size of the TC events in the ADM and SDM. This limitation can be addressed by defining the extremes using the Peaks Over Threshold approach. Additionally, I have also not explored the roles of large-scale climate variability such as ENSO and PDO on the observed trends. However, results from this study have a significant impact on environmental and infrastructural assessment as well as disaster risk management. Changes in the upper tails of extreme precipitation distributions caused by TCs often cause great climate disasters. In addition to flooding, these storms cause further damage from their strong winds, and storm surges for coastal areas. The expected changes in the upper quantiles of TC-induced extreme precipitation events has stark implications for the design of infrastructure and buildings, for the management of landscapes that must be resilient to peak flows, and for planning how emergency responders act in rainstorm events. For example, the expected changes in the upper quantiles of TC-induced extreme precipitation should encourage municipal officials to revisit the traditional precipitation frequency analysis (used for hydrologic design) based on the assumption that precipitation records are generated by a single weather system and to consider the extreme precipitation distribution as a mixed population (of TC and non-TC precipitation) that weighs the individual precipitation-generating phenomenon appropriately.

Funding: This research received no external funding.

Conflicts of Interest: The authors declare no conflict of interest.

Appendix A

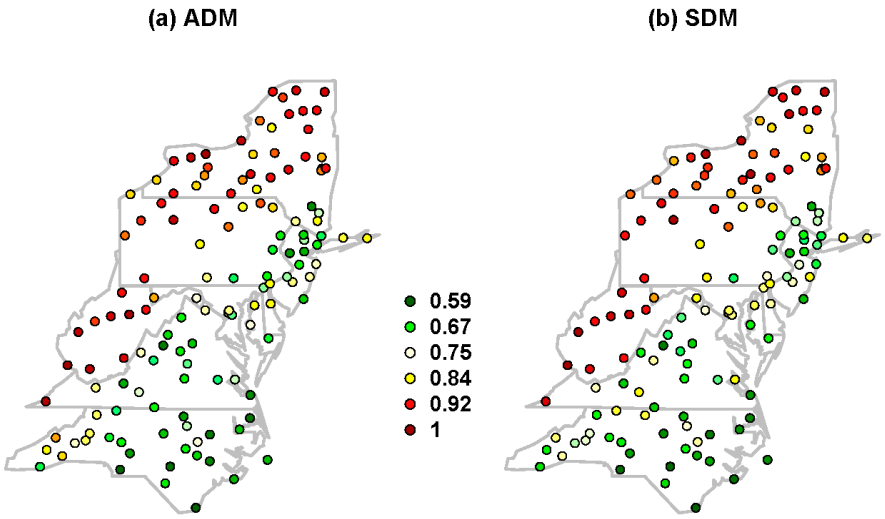

Figure A1. Frequency of non-TC extreme precipitation series for (**a**) ADM and (**b**) SDM.

References

1. Changnon, S.A. Assessment of flood losses in the United States. *J. Contemp. Water Res. Educ.* **2008**, *138*, 38–44. [CrossRef]
2. Lin, N.; Smith, J.A.; Villarini, G.; Marchok, T.P.; Baeck, M.L. Modeling extreme rainfall, winds, and surge from Hurricane Isabel (2003). *Weather Forecast.* **2010**, *25*, 1342–1361. [CrossRef]
3. Rappaport, E.N. Loss of life in the United States associated with recent Atlantic tropical cyclones. *Bull. Am. Meteorol. Soc.* **2000**, *81*, 2065–2073. [CrossRef]
4. Rappaport, E.N. Fatalities in the United States from Atlantic tropical cyclones: New data and interpretation. *Bull. Am. Meteorol. Soc.* **2014**, *95*, 341–346. [CrossRef]
5. Villarini, G.; Goska, R.; Smith, J.A.; Vecchi, G.A. North Atlantic tropical cyclones and US flooding. *Bull. Am. Meteorol. Soc.* **2014**, *95*, 1381–1388. [CrossRef]

6. Klotzbach, P.; Bowen, S.G.; Pielke, R.; Bell, M. Continental United States Hurricane Landfall Frequency and Associated Damage: Observations and Future Risks. *Bull. Amer. Meteor. Soc.* **2018**. [CrossRef]
7. Douglas, E.; Jacobs, J.; Hayhoe, K.; Silka, L.; Daniel, J.; Collins, M.; Wake, C. Progress and challenges in incorporating climate change information into transportation research and design. *J. Infrastruct. Syst.* **2017**, *23*, 04017018. [CrossRef]
8. Kunkel, K.E.; Easterling, D.R.; Kristovich, D.A.; Gleason, B.; Stoecker, L.; Smith, R. Recent increases in US heavy precipitation associated with tropical cyclones. *Geophys. Res. Lett.* **2010**, *37*. [CrossRef]
9. Barlow, M. Influence of hurricane-related activity on North American extreme precipitation. *Geophys. Res. Lett.* **2011**, *38*. [CrossRef]
10. Keim, B.D.; Robbins, K.D. Occurrence dates of North Atlantic tropical storms and hurricanes: 2005 in perspective. *Geophys. Res. Lett.* **2006**, *33*. [CrossRef]
11. Bove, M.C.; O'Brien, J.J.; Eisner, J.B.; Landsea, C.W.; Niu, X. Effect of El Niño on US landfalling hurricanes, revisited. *Bull. Am. Meteorol. Soc.* **1998**, *79*, 2477–2482. [CrossRef]
12. Nogueira, R.C.; Keim, B.D. Annual volume and area variations in tropical cyclone rainfall over the eastern United States. *J. Clim.* **2010**, *23*, 4363–4374. [CrossRef]
13. Landsea, C.W.; Pielke Jr, R.A.; Mestas-Nunez, A.M.; Knaff, J.A. Atlantic basin hurricanes: Indices of climatic changes. *Clim. Change* **1999**, *42*, 89–129. [CrossRef]
14. Webster, P.J.; Holland, G.J.; Curry, J.A.; Chang, H.-R. Changes in tropical cyclone number and intensity in a warming environment. *Science* **2005**, *309*, 1844–1846. [CrossRef] [PubMed]
15. Emanuel, K.A. Increasing destructiveness of tropical cyclones over the past 30 years. *Nature* **2005**, *326*, 686–688. [CrossRef] [PubMed]
16. Klotzbach, P.J. Trends in global tropical cyclone activity over the past twenty years (1986–2005). *Geophys. Res. Lett.* **2006**, *33*. [CrossRef]
17. Elsner, J.B.; Kossin, J.P.; Jagger, T.H. The increasing intensity of the strongest tropical cyclones. *Nature* **2008**, *455*, 92–95. [CrossRef] [PubMed]
18. Shepherd, J.M.; Grundstein, A.; Mote, T.L. Quantifying the contribution of tropical cyclones to extreme rainfall along the coastal southeastern United States. *Geophys. Res. Lett.* **2007**, *34*. [CrossRef]
19. Lau, K.M.; Zhou, Y.P.; Wu, H.T. Have tropical cyclones been feeding more extreme rainfall? *J. Geophys. Res.: Atmos.* **2008**, *113*. [CrossRef]
20. Knight, D.B.; Davis, R.E. Contribution of tropical cyclones to extreme rainfall events in the southeastern United States. *J. Geophys. Res.: Atmos.* **2009**, *114*. [CrossRef]
21. Groisman, P.Y.; Knight, R.W.; Karl, T.R.; Easterling, D.R.; Sun, B.; Lawrimore, J.H. Contemporary changes of the hydrological cycle over the contiguous United States: Trends derived from in situ observations. *J. Hydrometeorol.* **2004**, *5*, 64–85. [CrossRef]
22. Zhu, L.; Quiring, S.M. Variations in tropical cyclone precipitation in Texas (1950 to 2009). *J. Geophys. Res. Atmos.* **2013**, *118*, 3085–3096. [CrossRef]
23. Agel, L.; Barlow, M.; Qian, J.H.; Colby, F.; Douglas, E.; Eichler, T. Climatology of daily precipitation and extreme precipitation events in the northeast United States. *J. Hydrometeorol.* **2015**, *16*, 2537–2557. [CrossRef]
24. Interagency Committee on Water Data (IACWD) (1982) Guidelines for Determining Flood Flow Frequency: Bulletin 17-B. Available online: https://www.fema.gov/media-library-data/20130726-1553-20490-9670/dl_flow.pdf (accessed on 8 May 2019).
25. IPCC. *Managing the Risks of Extreme Events and Disasters to Advance Climate Change Adaptation: Special Report of the Intergovernmental Panel on Climate Change*; Field, C.B., Barros, V., Stocker, T.F., Qin, D., Dokken, D.J., Ebi, K.L., Mastrandrea, M.D., Mach, K.J., Plattner, G.-K., Allen, S.K., et al., Eds.; Cambridge University Press: Cambridge, UK, 2012; p. 582.
26. Koenker, R. *Quantile Regression*; Cambridge University Press: Cambridge, UK, 2005.
27. Koenker, R.; Quantreg: Quantile Regression. R package version 5.05. R Foundation, for Statistical Computing: Vienna) 2013. Available online: http://CRAN.R-project.org/package=quantreg (accessed on 8 May 2019).
28. Dhakal, N.; Tharu, B. Spatiotemporal trends in daily precipitation extremes and their connection with North Atlantic tropical cyclones for the Southeastern United States. *Int. J. Climatol.* **2018**. [CrossRef]

29. Ying, M.; Chen, B.; Wu, G. Climate trends in tropical cyclone-induced wind and precipitation over mainland China. *Geophys. Res. Lett.* **2011**, *38*, L01702. [CrossRef]
30. Hernandez; Ayala, J.J.; Matyas, C.J. Spatial distribution of tropical cyclone rainfall and its contribution to the climatology of Puerto Rico. *Phys. Geogr.* **2017**, *39*, 1–20. [CrossRef]
31. National Climate Assessment. US Global Change Research Program. Available online: http://nca2014.globalchange.gov/ (accessed on 27 January 2019).
32. Polsky, C.; Allard, J.; Crane, R.; Yarnal, B. The Mid-Atlantic Region and its climate: Past, present, and future. *Clim. Res.* **2000**, *4*, 161–173. [CrossRef]
33. Easterling, D.R.; Peterson, T.C.; Karl, T.R. On the development and use of homogenized climate datasets. *J. Clim.* **1996**, *9*, 1429–1434. [CrossRef]
34. Jarvinen, B.R.; Neumann, C.J.; Davis, M.A.S. *A Tropical Cyclone Data Tape for the North Atlantic Basin, 1886–1983: Contents, Limitations, and Uses*; NOAA Tech. Memo., NWS NHC: Miami, FL, USA, 1984.
35. Barbosa, S.M. Quantile trends in Baltic sea level. *Geophys. Res. Lett.* **2008**, *35*. [CrossRef]
36. Efron, B.; Tibshirani, R.J. *An Introduction to the Bootstrap*; Chapman & Hall/ CRC (Monographs on Statistics & Applied Probability): London, UK, 1994.
37. Galvao, A.F.; Montes-Rojas, G. On bootstrap inference for quantile regression panel data: A monte carlo study. *Econometrics* **2015**, *3*, 654–666. [CrossRef]
38. Fan, L.; Chen, D. Trends in extreme precipitation indices across China detected using quantile regression. *Atmos. Sci. Lett.* **2016**, *17*, 400–406. [CrossRef]
39. Tan, X.; Shao, D. Precipitation trends and teleconnections identified using quantile regressions over Xinjiang, China. *Int. J. Climatol.* **2017**, *37*, 1510–1525. [CrossRef]
40. Jenkinson, A.F. The frequency distribution of the annual maximum (or minimum) of meteorological elements. *Q. J. R. Meteorol. Soc.* **1955**, *81*, 158–171. [CrossRef]
41. Coles, S. *An Introduction to Statistical Modeling of Extreme Values*; Springer: London, UK, 2001.
42. DeGaetano, A.T. Time-dependent changes in extreme-precipitation return-period amounts in the continental United States. *J. Appl. Meteorol. Climatol.* **2009**, *48*, 2086–2099. [CrossRef]
43. Kharin, V.V.; Zwiers, F.W. Estimating extremes in transient climate change simulations. *J. Clim.* **2005**, *18*, 1156–1173. [CrossRef]
44. Smith, R.L.; Naylor, J.C. A comparison of maximum likelihood and Bayesian estimators for the three-parameter Weibull distribution. *Appl. Stat.* **1987**, *36*, 358–369. [CrossRef]
45. Mishra, A.K.; Singh, V.P. Changes in extreme precipitation in Texas. *J. Geophys. Res.: Atmos.* **2010**, *115*. [CrossRef]
46. Cry, G.W. *Effects of Tropical Cyclone Rainfall on the Distribution of Precipitation over the Eastern and Southern United States*; Professional Paper 1; United States Department of Commerce, Environmental Sciences Services Administration: Rockville, MD, USA, 1967; p. 67.
47. Englehart, P.J.; Douglas, A.V. The role of eastern North Pacific tropical storms in the rainfall climatology of western Mexico. *Int. J.Climatol.* **2001**, *21*, 1357–1370. [CrossRef]
48. Nogueira, R.C.; Keim, B.D.; Brown, D.P.; Robbins, K.D. Variability of rainfall from tropical cyclones in the eastern USA and its association to the AMO and ENSO. *Theor. Appl. Climatol.* **2013**, *112*, 273–283. [CrossRef]
49. Rodgers, E.B.; Adler, R.F.; Pierce, H.F. Contribution of tropical cyclones to the North Pacific climatological rainfall as observed from satellites. *J.Appl. Meteorol.* **2000**, *39*, 1658–1678. [CrossRef]
50. Rodgers, E.B.; Adler, R.F.; Pierce, H.F. Contribution of tropical cyclones to the North Atlantic climatological rainfall as observed from satellites. *J.Appl. Meteorol.* **2001**, *40*, 1785–1800. [CrossRef]
51. Jiang, H.; Zipser, E.J. Contribution of tropical cyclones to the global precipitation from eight seasons of TRMM data: Regional, seasonal, and interannual variations. *J. Clim.* **2010**, *23*, 1526–1543. [CrossRef]
52. Wright, D.B.; Knutson, T.R.; Smith, J.A. Regional climate model projections of rainfall from US landfalling tropical cyclones. *Clim. Dyn.* **2015**, *45*, 3365–3379. [CrossRef]
53. Hirschboeck, K.K. Climate and floods. *Natl. Water Summ.* **1988**, *89*, 67–88.
54. Son, C.; Lee, T.; Kwon, H.H. Integrating nonstationary behaviors of typhoon and non-typhoon extreme rainfall events in East Asia. *Sci. Rep.* **2017**, *7*, 5097. [CrossRef]
55. Rossi, F.; Fiorentino, M.; Versace, P. Two-component extreme value distribution for flood frequency analysis. *Water Resour. Res.* **1984**, *20*, 847–856. [CrossRef]

56. Waylen, P.; Woo, M.K. Prediction of annual floods generated by mixed processes. *Water Resour. Res.* **1982**, *18*, 1283–1286. [CrossRef]
57. Walsh, K.J.E.; McBride, J.L.; Klotzbach, P.J.; Balachandran, S.; Camargo, S.J.; Holland, G.; Knutson, T.R.; Kossin, J.P.; Lee, T.-C.; Sobel, A.; et al. Tropical cyclones and climate change. *WIREs Clim. Change* **2016**, *7*, 65–89. [CrossRef]